Experimental Investigation of the Accuracy of an Ultrawideband Time-Domain Microwave-Tomographic System

Experimental Investigation on the Accuracy of an Ultra-Wideband Time Domain Microwave Tomography System

Xuezhi Zeng, *Student Member, IEEE,* Andreas Fhager, *Member, IEEE,* Peter Linner, *Life Senior Member, IEEE,* Mikael Persson, *Member, IEEE,* and Herbert Zirath, *Fellow, IEEE*

***Abstract*—The measurement accuracy of an ultra-wideband time domain microwave tomography system is investigated. In order to make an assessment of the random variation of the measurements, the measurement repeatability of the system is evaluated by comparison with an ultra-wideband frequency domain system. A phantom is imaged with the time domain microwave tomography system and the reconstructed images are compared to those obtained by using the frequency domain system. The results suggest that with averaging tens of measurements, the time domain system can achieve the same level of measurement repeatability as that of the frequency domain system in the interesting frequency range of microwave tomography. The imaging results, however, indicate that the phantom reconstruction does not require such high measurement accuracy. The permittivity profile of the phantom reconstructed from the non-averaging time domain measurements is very similar to that obtained by means of the frequency domain system.**

***Index Terms*—Time domain measurements, Microwave imaging, Microwave measurements, Measurement errors, Random noise, Oscilloscopes.**

I. Introduction

Microwave tomography is an approach to active microwave imaging which poses an inverse scattering problem. In microwave tomography, several transmitters illuminate an object-under-test from different directions and the scattered field is measured at several different locations. By utilizing the received signals, the dielectric properties of the object are then quantitatively reconstructed.

The biomedical applications of microwave tomography have been explored extensively in the past few decades [1]–[3]. It has been shown that the dielectric properties of a biological tissue are strongly dependent on its physiological and pathological conditions [4]–[8]. Therefore, with microwave tomography, biological tissues can be differentiated based on the differences in their dielectric properties.

A microwave tomography reconstruction is generally achieved by minimizing the difference between measured data and computed data by updating the dielectric properties. In the last few years, various types of reconstruction algorithms have been investigated for microwave tomography. These include methods based on mono-frequency, multiple frequencies and time domain data [9]–[16]. In contrast with the former two types of methods, which use object information at a single frequency [9]–[11] or at a few discrete frequencies [12]–[13] in reconstructions, a reconstruction algorithm based on time domain data employs the scattered field of an object over an entire wideband [14]–[16]. Our previous work showed that, by the use of time domain data, the reconstructions presented very good quality with high resolution and high accuracy [14]–[15]. The efficacy of the time domain reconstructions for assessing a breast's internal composition was demonstrated in the most recent work [16].

Time domain data is often obtained with the help of a vector network analyzer (VNA) [17]–[18]. By using the VNA, scattering parameters at a large number of discrete frequencies are measured, and the collected frequency domain data is then utilized to synthesize time domain signals. This approach is widely employed in microwave imaging in order to obtain scattered signals in time domain [14], [19]–[21]. With such a measurement strategy, the acquisition of the time domain data is time consuming due to the required frequency sweeping. In comparison with an ultra-wideband (UWB) frequency domain system (e.g., a VNA), a UWB time domain system has the advantage of fast acquisition of time domain data, which is preferable for clinical applications.

The measurement accuracy of a microwave tomography system is essential to image reconstructions. Compared with a frequency domain system, a time domain system has a lower signal to noise ratio, which may degrade reconstruction quality depending on the sensitivity of microwave tomography reconstructions to measurement error. In [22], a time domain UWB radar system was investigated for tomographic imaging. A plastic pipe and a metallic cylinder were imaged at high resolution and the system showed a high potential for nondestructive evaluation. However, no relevant work was carried out on investigating whether the reconstructed images were degraded due to the lower measurement accuracy of the time domain system, in comparison to a frequency domain system.

As little research has been conducted addressing this problem, the aim of this paper is to investigate the measurement accuracy of a UWB time domain system for microwave tomography. The investigation is carried out experimentally by comparison with a UWB frequency domain system. With a view to estimating the random error of the time domain system, the standard deviations of time domain measurements, under repeatability conditions, are calculated and compared

X. Zeng, A. Fhager and M. Persson are with the Department of Signals and Systems, Chalmers University of Technology, Gothenburg, SE412-96 Sweden.

P. Linner and H. Zirath are with Microwave Electronics Laboratory, Chalmers University of Technology, Gothenburg, SE412-96, Sweden.

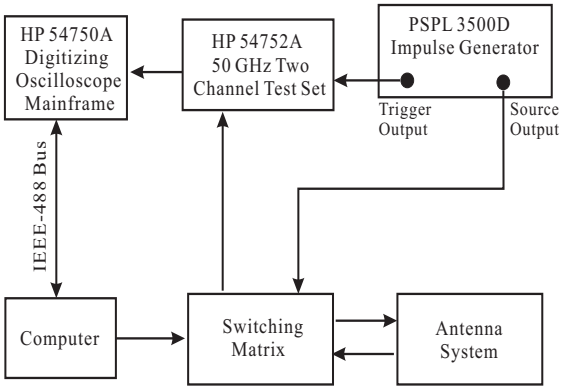

Fig. 1. The block diagram of the ultra-wideband time domain microwave tomography system.

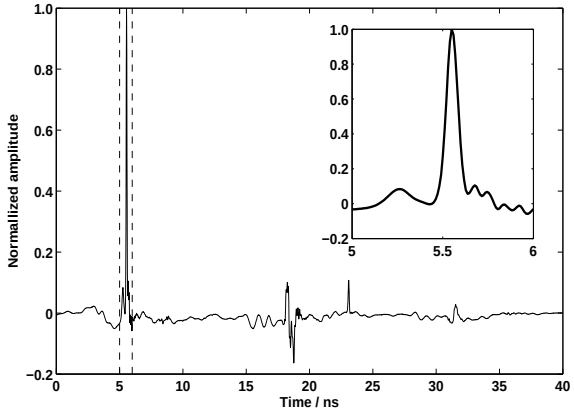

Fig. 2. The output waveform of the impulse generator.

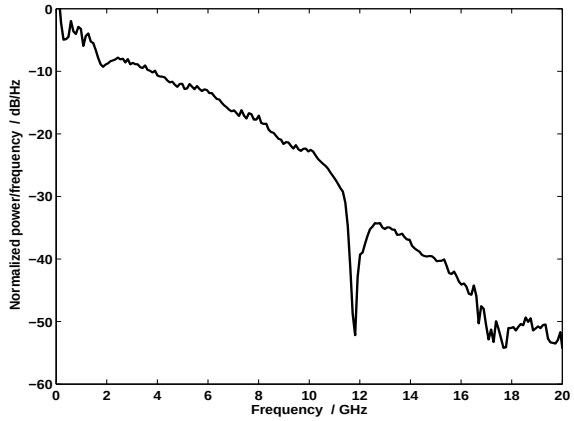

Fig. 3. The power spectrum of the impulse generator output.

to those of frequency domain measurements. Then, in order to examine whether the time domain system is accurate enough for microwave tomography reconstructions, a phantom is imaged with the system and the reconstructed images are compared to those obtained by using the frequency domain system.

II. Ultra-wideband time domain experimental system for microwave tomography

Fig. 1 shows the system block diagram of the UWB time domain microwave tomography system. The experimental system mainly comprises an impulse generator, a sampling oscilloscope, an antenna array and a switching matrix. The sampling oscilloscope is composed of a mainframe and a wideband two channel test set.

With this measurement system, an impulse signal generated by the impulse generator is transmitted by one of the antennas into an object-under-test, and the scattered field is acquired by the remaining antennas. The acquired signals are sampled and digitized by means of the sampling oscilloscope. This process is repeated until all the antennas have been used for transmitting. The switching matrix is employed in order to select different transmitting and receiving antenna pairs. The synchronization of the transmitter and receiver modules is achieved by connecting the trigger output of the impulse generator to the trigger input of the two channel test set. The whole measurement is automated with the help of a personal computer, via the IEEE-488 bus. The hardware of the experimental system is described in detail below.

A. Impulse Generator

The model 3500D impulse generator of Picosecond Pulse Lab (PSPL) produces fast impulses with full width at half maximum (FWHM) duration of about 75 picoseconds (ps). Connecting the impulse generator to the sampling oscilloscope with a coaxial cable, we measured the output signal of the impulse generator. The recorded waveform was shown in Fig. 2 and its power spectrum was presented in Fig. 3. It is seen that the output waveform includes an impulse and baseline perturbations, which occur about 10 nanoseconds (ns) after the impulse. The enlarged impulse is shown in the inset figure. The power spectrum differs from that of an ideal Gaussian impulse; the difference is largely attributed to the presence of the perturbations.

The peak amplitude of the generator output is larger than 8 V with selectable positive or negative polarity. The impulse amplitude may be adjusted by two microwave-quality step attenuators, over a 0 to 81 dB range in 1 dB steps. The output impedance of the generator is well matched to 50 ohm to absorb reflections from mismatch loads. A baseline offset circuit provides adjustable offset to $\pm$ 5 V. The repetition rate of the generator can be set from 10 Hz to 1 MHz and the delay from the trigger output to the impulse output is adjustable from 0 ns to 110 ns in 10 ns increments. The time jitter of the impulse generator σ_s is about 1.5 ps root mean square (rms) [23].

B. Antenna System

Twenty monopole antennas are evenly distributed in a circle with a radius of ten centimeters and an object-under-test is put in the imaging region surrounded by the antenna

array. A monopole has a relatively narrow bandwidth in air, however when placed in a lossy medium, its bandwidth increases significantly with the associated resistive loading [24]. The main reason for using the monopole is its simple structure, which can be easily and accurately modeled in a computational program. In addition, monopoles can be positioned in close proximity to the imaging target, with high-element density when configured in an imaging array. Monopoles are also cheap and easy to manufacture. A mechanical switching matrix is used for changing the transmitting and receiving antennas.

C. Data Acquisition Module

The scattered signal of an object-under-test is measured with the help of the Hewlett-Packard (HP) 54750A digitizing oscilloscope main frame and the 50 GHz two channel test HP 54752A. Equivalent time sampling technique [25] is employed in the oscilloscope in order to extend the effective sample rate of the analog to digital converter (ADC), and with this technique the time interval resolution can be as high as 62.5 femtoseconds (fs) [26]. The input of the sampling oscilloscope is limited by the ADC and its input dynamic range is $\pm$ 400 mV.

III. Measurement Repeatability

A. Error Analysis

Time domain measurements are subject to unavoidable errors, and various types of error sources of a sampling oscilloscope have been studied in the literature [27]–[32]. In general, the error sources can be divided into systematic errors and random errors. The systematic errors can be calibrated out [28]–[29], and it is mainly the random errors which may affect reconstruction quality.

The random errors of the time domain system consist of a horizontal part and a vertical part [28]. The random error presented in the horizontal axis is a time jitter, which causes inaccurate sampling instants. The vertical random errors are thermal noise and quantization noise; the latter is usually much smaller due to the high resolution of the ADC.

The way the random errors affecting a time domain measurement can be described by the following equation:

$$y_j = x(t_j + \tau_j) + \varepsilon_j + \gamma_j \tag{1}$$

where y_j is the jth sample of a measured signal $y(t)$, $x(t)$ is the true voltage signal, t_j is the ideal sampling instant of the jth sample and τ_j is the random time jitter. ε_j represents the thermal noise and γ_j is the quantization noise. We assume that the jitter and additive noise are independent zero-mean random variables.

The random variation of time domain measurements can be characterized by measurement repeatability, which may be expressed quantitatively in terms of the standard deviation of measurements under repeatability conditions:

$$\sigma_{Rep_k}(f) = \sqrt{\frac{1}{N}\sum_{i=1}^{N}(Y_{ik}(f) - \overline{Y_k(f)})^2} \tag{2}$$

Here N is the number of repeated measurements, $Y_{ik}(f)$ is the fast Fourier transform (FFT) of the acquired waveform of index i. $\overline{Y_k(f)}$ is the average of the FFT of all acquired waveforms. $Y_{ik}(f)$ and $\overline{Y_k(f)}$ are either amplitudes in volts (when $k = 1$) or phases in degrees (when $k = 2$).

The amplitude repeatability is usually expressed as a relative value. Defining signal-to-noise ratio $\text{SNR}(f) = \overline{Y_1(f)}/\sigma_{Rep_1}(f)$, we express the amplitude repeatability in the unit dB:

$$\sigma_{Rep}^{dB}(f) = 20 \cdot \log_{10}[1 + \frac{1}{\text{SNR}(f)}] \tag{3}$$

When SNR increases, the amplitude repeatability error σ_{Rep}^{dB} becomes smaller. It is a well known fact that the error angle is proportional to the relative noise level [33], therefore the phase repeatability error σ_{Rep_2} also decreases with SNR.

It is usually assumed that, up on averaging, the time jitter acts as a Gaussian low pass filter [27], so that the amplitude spectrum of the average signal, $\overline{Y_1(f)}$, can be expressed as:

$$\overline{Y_1(f)} = |X_{in}(f)| \cdot |H(f)| \cdot P(f) \tag{4}$$

where $X_{in}(f)$ is the frequency spectrum of the input signal of the oscilloscope, and $H(f)$ is the frequency response of the oscilloscope, which exhibits a low-pass filtering characteristic. $P(f)$ is the Fourier transform of the jitter's probability density function and it has the following expression [34]:

$$P(f) = e^{-0.5*(2\pi f \cdot \sigma_t)^2} \tag{5}$$

where σ_t is the standard deviation of time jitter in seconds. The effects of jitter can then be removed by means of deconvolution.

For the time domain microwave tomography system presented in Fig. 1, the frequency spectrum of the oscilloscope's input can be expressed as follows:

$$X_{in}(f) = I(f) \cdot TR(f) \tag{6}$$

where $I(f)$ is the frequency spectrum of the output signal of the impulse generator, and $TR(f)$ is the transfer function between the impulse generator and sampling oscilloscope, which comprises the frequency response of the transmitting and receiving antennas and the signal propagation effects.

As a result, the measurement repeatability of the time domain system is dependent on the performance of the antenna and the properties of imaged objects. The narrowband characteristic of the monopole antenna limits the bandwidth of the time domain system. In order to investigate the measurement repeatability of the time domain system in the interesting frequency range of microwave tomography (from a few hundred megahertz to several gigahertz), a general evaluation is made below disregarding the effects of the antennas and propagation.

B. Measurements

Repeated measurements are carried out in order to evaluate the measurement repeatability of the time domain system and the evaluation is made by comparison with an ultra-wideband frequency domain system.

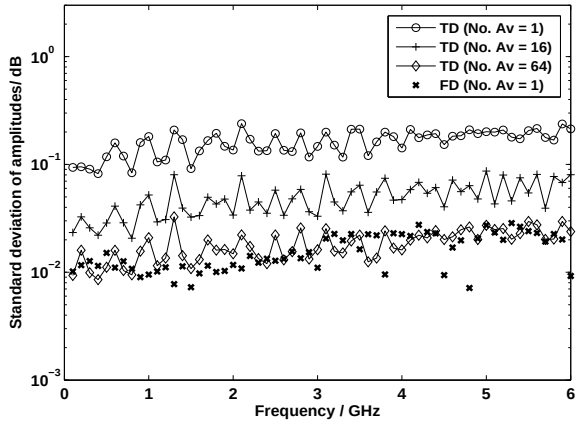

(a)

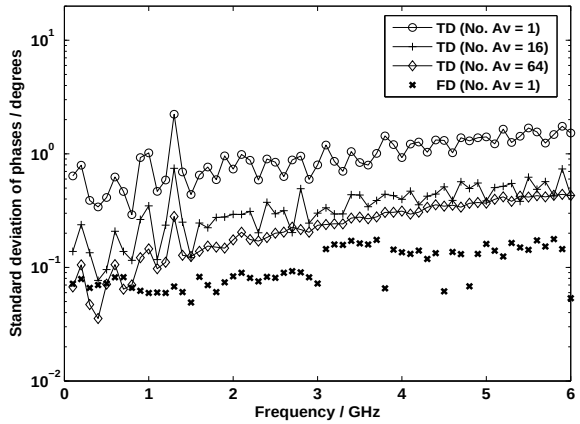

(b)

Fig. 4. The repeatability standard deviations of the (a) spectral amplitudes and (b) phases of the measured time domain signal in comparison with those of the transmission coefficients obtained with the VNA. The measured time domain signal was a maximum input of the oscilloscope and the transmission coefficient was about 0 dB. The lines with circle, plus and diamond markers represent the time domain measurement results when the number of average is 1, 16 and 64 respectively. The frequency domain measurement results are shown as multiply markers.

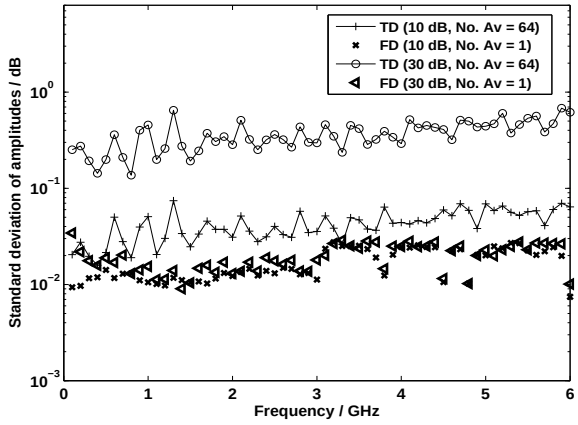

(a)

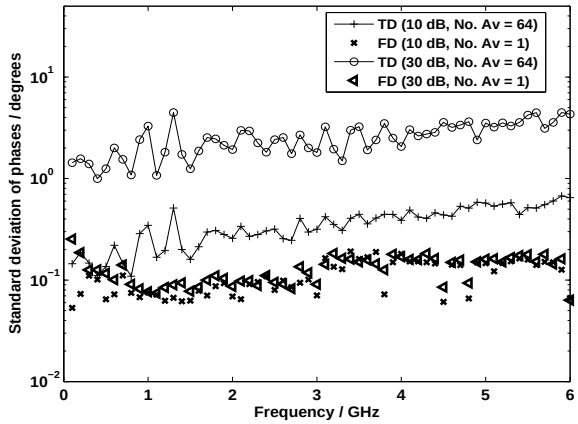

(b)

Fig. 5. The repeatability standard deviations of the (a) spectral amplitudes and (b) phases of the measured time domain signals in comparison with those of the transmission coefficients obtained with the VNA. The lines with plus and circle markers represent the time domain measurement results when the attenuator connected between the impulse generator and the oscilloscope has insertion loss of 10 dB and 30 dB respectively. The repeatability standard deviations of the transmission coefficients are shown as multiply makers and left triangle markers when the attenuator connected between the ports of the VNA has insertion loss of 10 dB and 30 dB respectively.

1) Measurement Repeatability for a Maximum Input: As mentioned in section II-C, the oscilloscope has an input limit. We will first estimate the measurement repeatability of the time domain system when the oscilloscope has a maximum input.

The impulse generator was connected to the oscilloscope with a high performance coaxial cable. The output of the impulse generator was adjusted to 28 dB below the maximum output in order to make the input signal of the oscilloscope just within its input dynamic range. N = 50 waveforms were recorded repetitively, and the measurements were performed three times with different numbers of average applied in the acquisition of each waveform. The repeatability errors of the amplitudes and phases of the measured signal were calculated according to eq. (2) and eq. (3), and the results are shown in Fig. 4. The data is presented from 100 MHz to 6 GHz, which covers the most interesting frequency range of microwave tomography. The lines with circle, plus, and diamond markers represent the results when the number of average is No. Av = 1, 16 and 64 respectively.

In order to make a comparison with a UWB frequency domain system, the measurement repeatability of frequency domain measurements performed with a VNA (PNA Series vector network analyzer E8362B) [35] were also calculated. Connecting the two ports of the VNA directly (under such condition, the transmission coefficient is about 0 dB), we measured the transmission coefficients at several different frequency points N = 50 times. The output power was set to 0 dBm and the intermediate frequency (IF) bandwidth was 35 kHz, which were the common settings of a VNA. The amplitude and phase repeatability of the transmission coefficients in frequency range 100 MHz to 6 GHz were calculated and the results are presented in Fig. 4 as multiply markers.

The results show that the amplitude repeatability error

of the time domain signal decreases with the number of average, while the phase repeatability change very little at some frequency points when the number of average increases from 16 to 64. It can be seen that when No. Av = 64, the amplitude repeatability of the time domain measurement is very close to that of the transmission coefficients measured with the VNA.

2) Measurement Repeatability for Different Input Levels: The measurement repeatability presented above was evaluated for a case when the sampling oscilloscope had a maximum input signal. It would also be of interest to investigate the measurement repeatability of the time domain system for different input levels. Keeping the previous settings of the time domain system, we connected two different wideband attenuators between the impulse generator and the oscilloscope respectively, and these two attenuators have insertion loss of 10 dB and 30 dB. For each case, N = 50 waveforms were acquired and the number of average was No. Av = 64 in the acquisition of each waveform. The repeatability standard deviations of the spectral amplitudes and phases of the measured signals are shown in Fig. 5 as the lines with plus and circle markers respectively.

These two attenuators were connected between the two ports of the VNA respectively, and the transmission coefficients were measured N = 50 times for each case. The repeatability standard deviations of the measured transmission coefficients, are shown in Fig. 5 as multiply markers and left triangle markers, when the attenuator connected between the ports of the VNA has insertion loss of 10 dB and 30 dB respectively.

It can be seen that both the amplitude and phase repeatability errors of the time domain measurements become larger as the input signal of the oscilloscope becomes weaker, which can be expected from the analysis made in section III-A. Unlike the time domain measurements, the frequency domain measurements have almost constant repeatability standard deviations as the transmission coefficient changes. These results indicate that as the strength of the received time domain signal becomes smaller, a larger number of average needs to be used in the measurements in order to achieve the same level of measurement repeatability as that of the frequency domain system.

An automatic gain control (AGC) technique can be utilized in order to improve the measurement repeatability of weak input signals. By using a variable gain amplifier ahead of the oscilloscope, weak inputs can be amplified to a specific level within the input dynamic range of the oscilloscope. The required gain is determined during a fast preliminary measurement.

Two additional terms, $\sqrt{G}$ and ξ_j, are added to the right hand side of eq. (1) in order to express a measured signal $e(t)$ when a variable gain amplifier is employed:

$$e_j = \sqrt{G} \cdot x(t_j + \tau_j) + \xi_j + \varepsilon_j + \gamma_j \tag{7}$$

where e_j is the jth sample of the measured signal $e(t)$. G is the power gain of the amplifier, and ξ_j is the noise contributed by the amplifier.

According to the above equation, the noise present in the measurement is the sum of the amplifier noise and the oscilloscope noise. Therefore, the repeatability standard deviation of the spectral amplitude of the measured signal becomes:

$$\sigma_{Rep_G}(f) \approx \sqrt{\sigma^2_{Rep_1}(f) + \sigma^2_{\xi}(f)} \tag{8}$$

where σ_{Rep_1} is defined in eq. (2), which indicates the noise contribution from the oscilloscope, and σ_ξ represents the noise contribution from the amplifier.

In section III-A, $\overline{Y_1(f)}$ represents the average amplitude spectrum of N repetitive measurements of $y(t)$. Here we denote by $\overline{E(f)}$ the average amplitude spectrum of N repetitive measurements of $e(t)$, then according to the definition SNR(f) made in section III-A, the signal-to-noise ratio (SNR$_G$) of the time domain measurement with the AGC technique applied is expressed as:

$$\text{SNR}_G(f) = \frac{\overline{E(f)}}{\sigma_{Rep_G}(f)} \tag{9}$$

Based on eq. (1) and eq. (7), it can be obtained that $\overline{E(f)} \approx \sqrt{G} \cdot \overline{Y_1(f)}$. Taking the ratio of SNR$_G(f)$ to SNR(f), we can evaluate the improvement of the signal-to-noise ratio by using the AGC technique:

$$\frac{\text{SNR}_G(f)}{\text{SNR}(f)} \approx \sqrt{G} \cdot \sqrt{\frac{\sigma^2_{Rep_1}(f)}{\sigma^2_{Rep_1}(f) + \sigma^2_{\xi}(f)}} \tag{10}$$

If the noise of the amplifier is negligible, the SNR improves about $\sqrt{G}$ times by the use of the AGC technique. This equation applies as long as the amplified signal is within the input dynamic range of the oscilloscope.

C. Theoretical Estimation of Measurement Repeatability

The measurement repeatability of the time domain system can be estimated analytically.

If the thermal noise and quantization noise are assumed to be white; this means that in the frequency domain, noise has a flat spectrum, the amplitude standard deviation $\sigma_{Rep_1}(f)$ can then be estimated from the following equation:

$$\sigma_{Rep_1}(f) = \sqrt{\frac{\sigma^2_Q}{f_s/2} + \frac{\sigma^2_T}{\text{BW}}} \cdot \sqrt{\frac{1}{\text{No.Av}}} \tag{11}$$

Here σ^2_Q and σ^2_T are the variances of quantization noise and thermal noise respectively. f_s is the effective sampling rate of the oscilloscope and BW is the effective noise bandwidth (ENB) of the oscilloscope. The -3 dB bandwidth of the oscilloscope is a good approximation of the ENB due to the sharp roll-off characteristic of its frequency response [36]. Averaging is routinely used during waveform acquisition in order to reduce the effects of additive noise. The improvement in the noise floor due to signal averaging is given approximately by the square root of the number of average No. Av.

The thermal noise of the oscilloscope is typically $\sigma_T \approx$ 0.75 mV rms [37] and the quantization noise power of the oscilloscope can be obtained from the following equation [38]:

$$\sigma^2_Q = \frac{(V_{p-p}/2^n)^2}{12} \tag{12}$$

Here V_{p-p} = 800 mV is the full scale input of the oscilloscope, n = 12 bits is the resolution of the ADC.

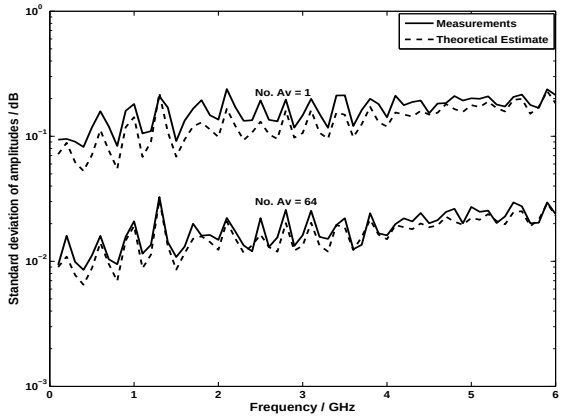

Fig. 6. Comparison of the amplitude repeatability errors obtained from measurements and theoretical estimation.

The -3 dB bandwidth of the oscilloscope is 50 GHz and the time interval resolution is 10 ps, which corresponds to an effective sampling rate f_s = 100 GHz. These parameters were used to estimate the repeatability standard deviation $\sigma_{Rep_1}(f)$ according to eq. (11). With the obtained value, the amplitude repeatability of the maximum input considered in section III-B1 was calculated according to eq. (3), and the obtained results are compared with the measurement results in Fig. 6 when No. Av = 1 and No. Av = 64.

It can be seen that good agreements are achieved between the theoretical estimates and the measurement results, which verifies the effectiveness of the theoretical estimation.

IV. Phantom Measurements and Reconstructions

The higher random variation of time domain measurements may produce distortions to microwave tomography reconstructions. In this section, a phantom is imaged by means of the time domain microwave tomography system and the reconstructed images are compared to those obtained by using the frequency domain system.

A. Reconstructions Made by means of the Time Domain and Frequency Domain Systems

A plastic cup of oil at the center of the imaging region was imaged by using the time domain microwave tomography system. The plastic cup was cylindrical-shaped, but with gradually increasing radius. The bottom diameter and top diameter of the cup were 55 mm and 70 mm respectively.

Measurements were performed according to the measurement procedure described in section II. Two groups of 20∗19 data sets were obtained when the number of average in the measurements was No. Av = 1 and 16 respectively. The same measurements were taken for an empty antenna system without the phantom, in order to carry out the calibration procedure of reconstructions [14]–[15].

With the phantom present, the signals acquired by antennas which are nearest and farthest from the transmitting antenna are shown in Fig. 7 when No. Av = 1. The recording length is 50 ns and 4096 sampling points are obtained. The responses

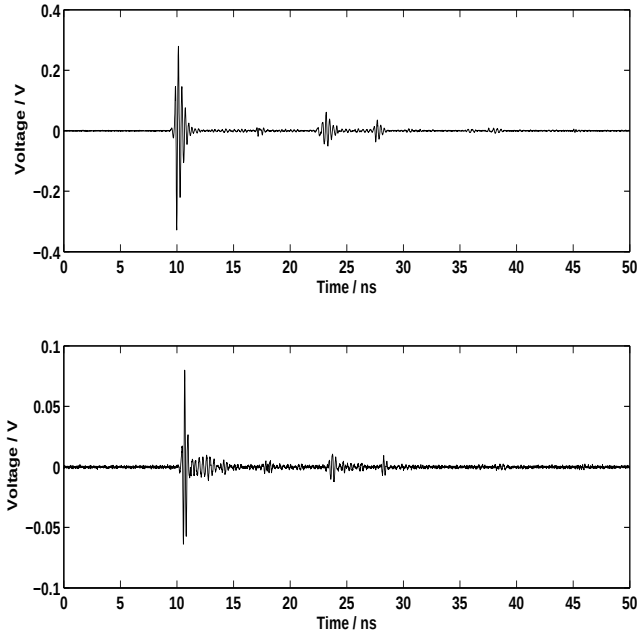

Fig. 7. The signals acquired by the antennas which are nearest (above) and farthest (below) from the transmitting antenna with the phantom present.

to the excitations of the impulse and the perturbations can be roughly identified by comparison to the output waveform of the impulse generator as shown in Fig. 2.

The recording lengths of signals should be carefully decided upon in the time domain measurements. As mentioned in section II-C, the time domain system is based on an equivalent time sampling technique, which constructs a waveform by accumulating samples over many wave cycles. As a result, the measurement time is determined by the recording length. A proper recording length should be chosen, on the one hand to make sure that the multiple scattered field of the object-under-test is collected, and on the other to make the measurement time as short as possible.

The dielectric properties of the phantom were reconstructed from the collected data by using a two dimensional time domain inversion algorithm, which was fully described in [14]. The reconstructed relative permittivity and conductivity profiles are presented in Fig. 8 (a), (b) and Fig. 9 (a), (b) respectively in comparison to those obtained by using the VNA in Fig. 8 (c) and Fig. 9 (c). The reconstructed region is a circle of radius 90 mm, with its center coinciding with the center of the antenna array. The color bar on the right of each image indicates the change of the relative permittivity or conductivity values. The scales of the relative permittivity or conductivity values are the same for all the pictures in order to clearly display the differences between the reconstructed images.

It is shown that the relative permittivity profiles reconstructed from the time domain measurements when No. Av = 1 and No. Av = 16 are very similar to that obtained from frequency domain measurements. Both the location and size of the cup are properly reconstructed in the relative permittivity

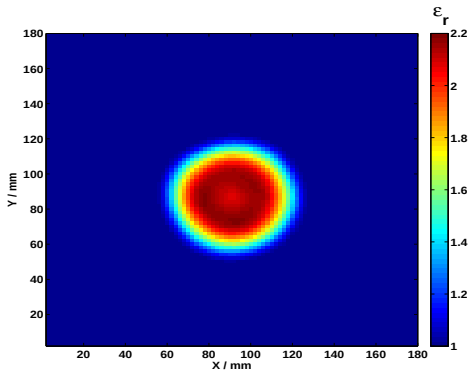

(a)

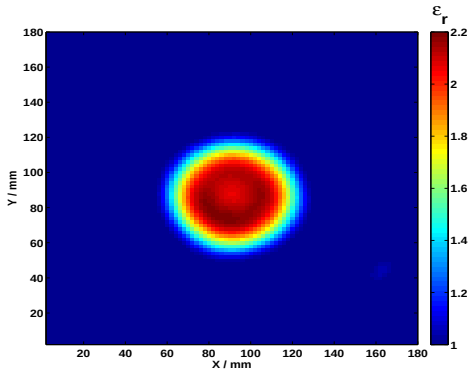

(b)

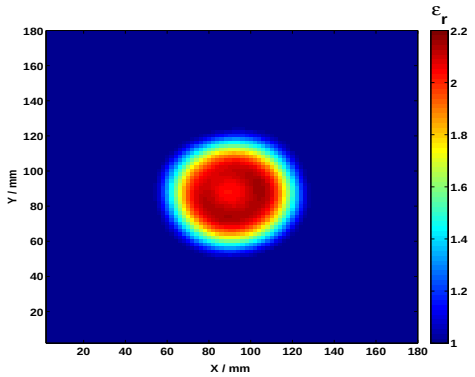

(c)

Fig. 8. The relative permittivity profiles of the phantom reconstructed from the (a) time domain measurements when No. Av = 1, (b) time domain measurements when No. Av = 16 and (c) frequency domain measurements.

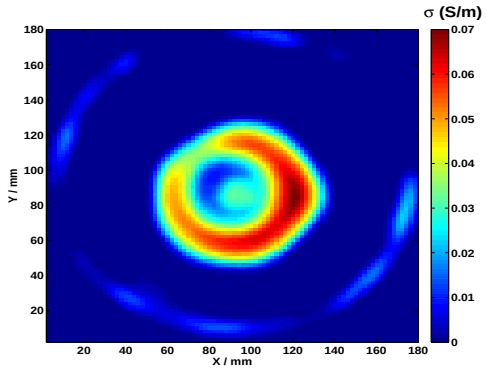

(a)

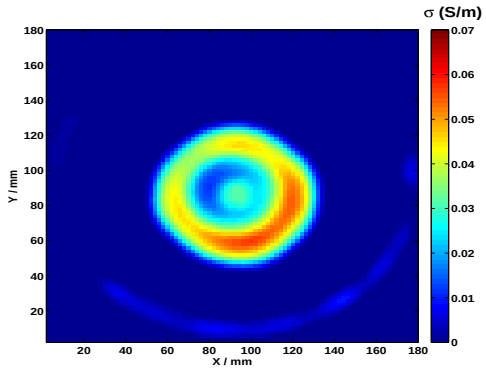

(b)

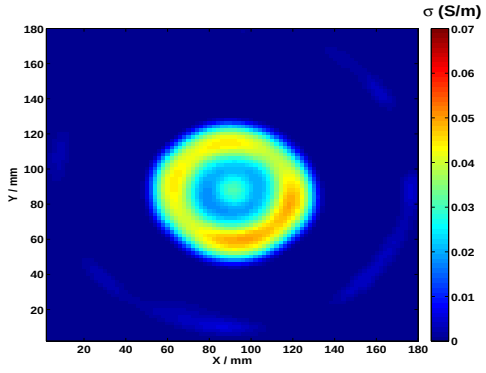

(c)

Fig. 9. The conductivity profiles(S/m) of the phantom reconstructed from the (a) time domain measurements when No. Av = 1, (b) time domain measurements when No. Av = 16 and (c) the frequency domain measurements.

profiles.

The conductivity profiles obtained from both the time domain and frequency domain measurements are not as reliable as the relative permittivity profiles, and holes appear in the reconstructed pictures. Comparing Fig. 9 (a) with Fig. 9 (c), it can be seen that the conductivity profile reconstructed from the time domain measurements when No. Av = 1 shows a larger variation of conductivity values and more artifacts than that obtained from the frequency domain measurements. The differences between the conductivity reconstructions made from the time domain and frequency domain measurements become smaller as the number of average increases in the time domain measurements, which can be seen by comparing Fig. 9 (b) with Fig. 9 (c).

The reason the conductivity reconstructions are worse, is that the imaginary part of the complex permittivity of the phantom is much smaller than the real part. Our previous work showed that the algorithm performs at its best when the real and imaginary parts are of the same size [14].

B. Reconstructions Made from Signals with Different Recording Lengths

The importance of choosing a proper recording length was discussed in the above subsection, and the influence of the recording length on the reconstructions is studied below.

Assuming the time instant when the signal is transmitted as the start of the recording time, then the recording length of a

time domain signal, T_R, can be determined by:

$$T_R = T_D + T_S \tag{13}$$

where T_D is the signal propagation time and T_S is the time duration of the signal itself.

In the microwave tomography system, the signal received by an antenna is the sum up of many signals, such as the direct wave from the transmitting antenna, the re-scattered wave from passive antennas and the multiple scattered waves. For the antenna which is farthest from the transmitting antenna, the propagation time of the direct wave can be approximately calculated:

$$T_D = \frac{D}{u_p} + \frac{L-D}{u_a} \tag{14}$$

where L = 20 cm is the diameter of the antenna array and $D \approx$ 7 cm is the diameter of the phantom. $u_p \approx c/\sqrt{\epsilon_r}$ and $u_a \approx c$ are the propagation velocity of the signal in the phantom and in air. $c = 3 \cdot 10^8$ m/s is the speed of light and according to the imaging results, the relative permittivity of the phantom is $\epsilon_r \approx 2.2$.

Inserting all the parameters into eq. (14), we calculate $T_D \approx 0.76$ ns. It can be seen from Fig. 7 that this value is a good estimate of the arrival time difference of the direct waves received by antennas which are respectively nearest and farthest from the transmitting antenna.

The rescattered waves from passive antennas and the multiple scattered waves arrive later at different time and the superposition of multiple path signals causes the broadening of the received signal. In addition, the antenna response also affects the time duration of the signal, T_S. It is well known that the time duration of a signal is inversely proportional to its bandwidth, therefore, the narrowband frequency response of the monopole antenna contributes to the extension of the signal duration. All these effects, together with the presence of the perturbations in the output of the impulse generator, make it difficult to choose a proper recording length. A good estimation of the recording length can be made from a fast preliminary measurement.

Referring to Fig. 7, instead of using the whole recorded signals of length 50 ns in the reconstructions, we used signals with recording lengths of 12 ns (from 6 ns to 18 ns) and 30 ns (from 6 ns to 36 ns) respectively to make reconstructions.

In order to compare the quality of reconstructions made from signals with different recording lengths, a relative reconstruction difference δ_{rec} is defined below:

$$\delta_{rec} = \frac{\iint_S [I_{TD}(x,y) - I_{FD}(x,y)]^2 \cdot ds}{\iint_S [I_{FD}(x,y)]^2 \cdot ds} \tag{15}$$

Where I_{TD} and I_{FD} represent the permittivity or conductivity profile reconstructed from time domain measurements and frequency domain measurements respectively. S is the two dimensional reconstructed region.

Fig. 10 shows the relative reconstruction differences as the number of iteration, for reconstructions made from signals with recording lengths of 12 ns, 30 ns and 50 ns respectively. It is shown that the relative reconstruction difference varies with the number of iteration within the first seven iterations and then keeps constant for the subsequent iterations. Therefore, at least seven iterations are required in the reconstructions. The presented results indicate that the reconstruction quality improves as the recording length increases from 12 ns to 30 ns, and this is because a 12 ns recording length is not long enough for collecting the multiple scattered field of the object. The results also suggest that as the recording length increases further to 50 ns, the reconstruction quality becomes worse, which could be attributed to unwanted late time arrival signals, for example, scattered signals from the surrounding environment.

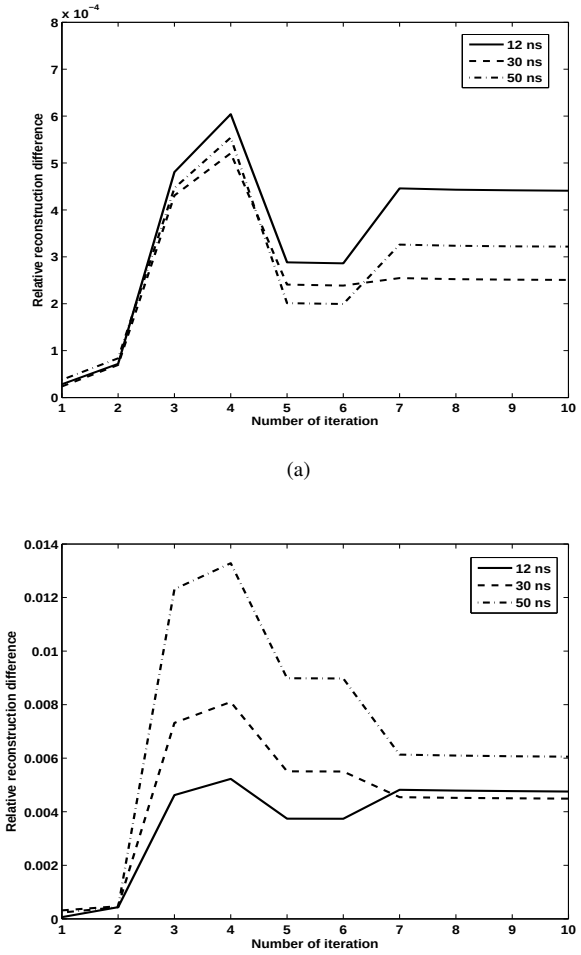

Fig. 10. The relative reconstruction differences of the (a) permittivity profiles and (b) conductivity profiles reconstructed from time signals with different recording lengths when No. Av = 1.

In summary, the quality of reconstructions made from time domain measurements is dependent on the recording length of time signals. In order to shorten the measurement time without much reduction in reconstruction quality, the perturbation level should be kept as small as possible.

V. Discussions

The effects of antennas and signal propagation were disregarded in the evaluation of the measurement repeatability of the time domain system. An antenna works as a bandpass

filter, and if taking the antenna response into account, the maximum input of the oscilloscope would have higher signal power spectral density in the interesting frequency range than the signal considered in section III-B1, because the signal power is distributed within a relatively narrower bandwidth. Therefore, better amplitude and phase repeatability can be expected due to the higher signal to noise ratio. In addition, different frequency components of the received signal suffer different levels of attenuation in the imaging medium, and the variation of the propagation loss versus frequency is dependent on the conductivity value of the imaging medium. This effect will cause a larger variation of the measurement repeatability versus frequency than that presented in section III-B.

The investigation in this paper is carried out for a specific time domain system. The highest signal to noise ratio of the time domain system is limited by the input dynamic range and noise power density of the oscilloscope. The oscilloscope used in this work has a typical noise level of 0.75 mV rms, and other sampling oscilloscopes with the same bandwidth and similar input dynamic range (the same or 25% larger) have typical noise levels varying from about 0.4 mV rms to 1 mV rms [37], [39]–[40]. Oscilloscopes with a smaller bandwidth (for example, 30 GHz) generally have lower noise power densities [37], [39]–[40]. These facts suggest that the results presented in this paper are of the general performance of UWB time domain systems.

The theoretical analysis presented in section III not only offers a way of estimating the measurement accuracy of a time domain system, but also is of great importance for designing a time domain system with certain measurement accuracy. According to the analysis, one way to increase the measurement accuracy is to reduce the noise level, which can be achieved by employing hardware with better noise performance or by the use of averaging. However, this method works at the cost of system expense or measurement speed. The other way for improving the SNR is to increase the signal power density in the interesting frequency range and this can be achieved by properly choosing the shape of transmitted pulse, transmitted power, antenna and switchable amplifier. Therefore, a proper system design, which compromises the system cost, measurement speed and measurement accuracy, can be proposed based on the theoretical analysis.

VI. Conclusion

The main purpose of this paper has been to evaluate the measurement accuracy of a UWB time domain system for microwave tomography by comparing it to a UWB frequency domain system.

The overall results indicate that although the random variation of time domain measurements is much larger than that of frequency domain measurements, the reconstructions of a phantom's permittivity made by means of the time domain and frequency domain systems agree well with each other. The conductivity profile of the phantom reconstructed from time domain measurements presents worse quality than that obtained from frequency domain measurements, and they are of less interests than the permittivity reconstructions due to the lower reliability.

Compared with a UWB frequency domain system, a UWB time domain system based on equivalent time sampling can be an order of magnitude faster and is also much more cost effective. The preliminary results reported would seem to indicate that UWB time domain systems have a higher potential for fast, economically viable microwave tomography than frequency domain systems. In the future, more complex measurement examples (for example, tissue phantoms immersed in matching liquid) will be considered in order to further verify the efficacy of the UWB time domain system.

Acknowledgment

This work was supported in part by VINNOVA within the VINN Excellence Center Chase, and in part by SSF within the Strategic Research Center Charmant.

References

[1] L. Jofre, M. S. Hawley, A. Broquetas, E. de los Reyes, M. Ferrando, and A. R. Elias-Fuste, "Medical imaging with a microwave tomographic scanner," *IEEE Trans. Biomed. Eng.,* vol. 37, no. 3, pp. 303–312, Mar. 1990.

[2] P. M. Meaney, M. W. Fanning, D. Li, S. P. Poplack, and K. D. Paulsen etc., "A clinical prototype for active microwave imaging of the breast," *IEEE Trans. Microwave Theory Tech.,* vol. 48, no. 11, pp. 1841–1853, Nov. 2000.

[3] S. Semenov, J. Kellam, P. Althausen, T. Williams, and A. Abubakar etc., "Microwave tomography for functional imaging of extremity soft tissues: feasibility assessment," *Phys. Med. Biol.,* vol. 52, no. 18, pp. 5705–5719, 2007.

[4] T. S. England and N. A. Sharples, "Dielectric properties of the human body in the microwave region of the spectrum," *Nature*, vol. 163, pp. 487–488, Mar. 1949.

[5] K. R. Foster and H. P. Schwan, "Dielectric properties of tissues and biological materials: A critical review," *Crit. Rev. Biomed. Eng.*, vol. 17, no. 1, pp. 25–104, 1989.

[6] C. Gabriel, S. Gabriel, and E. Corthout, "The dielectric properties of biological tissues: I. literature survey," *Phys. Med. Biol.*, vol.41, no. 11, pp. 2231–2249, 1996.

[7] S Gabriely, R W Lau and C Gabriel, "The dielectric properties of biological tissues: II. Measurements in the frequency range 10 Hz to 20 GHz," *Phys. Med. Biol.,* vol. 41, no. 11, pp.2251–2269, 1996.

[8] M. Lazebnik, D. Popovic, L. McCartney, C. Watkins, and etc., "A large scale study of the ultrawideband microwave dielectric properties of normal, benign and malignant breast tissues obtained from cancer surgeries," *Phys. Med. Biol.*, vol. 52, no. 20, pp. 6093–6115, 2007.

[9] S. Caorsi, G. L. Gragnani, and M. Pastorino, "Reconstruction of dielectric permittivity distributions in arbitrary 2-D inhomogeneous biological bodies by a multiview microwave numerical method," *IEEE Trans. Med. Imag.,* vol. 12, no. 2, pp. 232–239, Jun. 1993.

[10] Q. H. Liu, Z. Q. Zhang, T. T. Wang, J. A. Bryan, and G. A. Ybarra etc., "Active microwave imaging. I.- 2D forward and inverse scattering methods," *IEEE Trans, Microwave Theory Tech.,* vol. 50, no. 1, pp. 123–133, Jan. 2002.

[11] A. Abubakar, P. M. van den Berg, and J. J. Mallorqui, "Imaging of biomedical data using a multiplicative regularized contrast source inversion method," *IEEE Trans. Microwave Theory Tech.,* vol. 50, no. 7, pp. 1761–1771, Jul. 2002.

[12] W. C. Chew and J. H. Lin, "A frequency-hopping approach for microwave imaging of large inhomogeneous bodies," *IEEE Microwave Guided Wave Lett.*, vol. 5, no. 12, pp. 439–441, Dec. 1995.

[13] Q. Fang, P. M. Meaney, and K. D. Paulsen, "Microwave image reconstruction of tissue property dispersion characteristics utilizing multiple-frequency information," *IEEE Trans. Microwave Theory Tech.,* vol. 52, no. 8, pp. 1866–1875, Aug. 2004.

[14] A. Fhager, P. Hashemzadeh, and M. Persson, "Reconstruction quality and spectral content of an electromagnetic time-domain inversion algorithm," *IEEE Trans. Biomed. Eng.,* vol. 53, no. 8, pp. 1594–1604, Aug. 2006.

[15] A. Fhager and M. Persson, "Using a priori data to improve the reconstruction of small objects in microwave tomography,"*IEEE Trans. Microwave Theory Tech.,* vol. 55, no. 11. pp. 2454–2462, Nov. 2007.

[16] J. E. Johnson, T. Takenaka, and T. Tanaka, "Two-dimensional time-domain inverse scattering for quantitative analysis of breast composition," *IEEE Trans. Biomed. Eng.,* vol. 55, no. 8, pp. 1941–1945, Aug. 2008.

[17] M. E. Hines and H. E. Stinehelfer Sr., "Time domain oscillographic microwave network analysis using frequency domain data," *IEEE Trans. Microwave Theory Tech.,* vol. 22, no. 3, Mar. 1974.

[18] Z. A. Maricevic, T. K. Sarkar, Y. Hua and A. R. Djordjevic, "Time domain measurements with the Hewlett-Packard network analyzer HP8510 using the matrix pencil method," *IEEE Trans. Microwave Theory Tech.,* vol. 39, no. 3, pp.538–547, Mar. 1991.

[19] E. C. Fear, J. Sill and M. A. Stuchly, " Experimental feasibility study of confocal microwave imaging for breast tumor detection," *IEEE Trans. Microwave Theory Tech.,* vol. 49, pp. 887–892, March. 2003.

[20] X. Li, S. K. Davis, S. C. Hagness, D. W. van der Weide and B. D. Van Veen, " Microwave imaging via space-time beamforming: experimeal investigation of tumor detection in multilayer breast phantoms," *IEEE Trans. Microwave Theory Tech.,* vol. 52, no. 8, pp. 1856–1865, Aug.2004.

[21] M. Klemm, I. J. Craddock, J. A. Leendertz, A. Preece and R. Benjamin, "Radar-Based Breast Cancer Detection Using a Hemispherical Antenna Array–experimental Results," *IEEE Trans. Antennas Propagat.,* vol.57, no. 6, pp. 1692-1704, Jun. 2009.

[22] F. C. Chen and W. C. Chew, "Time domain ultra-wideband microwave imaging radar system," *J. of Electromagn. Waves and Appl.,* vol. 17, no. 2, pp. 313–331, 2003.

[23] Model 3500D Impulse Generator Instruction Manual. *Picosecond Pulse Lab.*

[24] C. J. Fox, P. M. Meaney, F. Shubitidze, L. Potwin, and K. D. Paulsen, "Characterization of an implicitly resistively-loaded monopole antenna in lossy liquid media," *International Journal of Antennas and Propagation,* vol. 2008, Article ID 580782, 2008.

[25] Application Note 1608: What is the difference between an equivalent time sampling oscilloscope and a real-time oscilloscope? *http://www.home.agilent.com/*

[26] 54750A User's Guide. *http://www.home.agilent.com/*

[27] W. L. Gans, " The measurement and deconvolution of time jitter in equivalent time waveform samplers," *IEEE Trans, Instrum, Meas.,* vol. IM-32, no. 1, pp.126–133, Mar. 1983.

[28] W. L. Gans, "Calibration and error analysis of a picosecond pulse waveform measurement system at NBS," *Proceedings of the IEEE,* vol. 74, no. 1, pp.86–90, Jan. 1986.

[29] J. Verspecht and K. Rush, "Individual characterization of broadband sampling oscilloscopes with a nose-to-nose calibration procedure," *IEEE Trans. Instrum. Meas.,* vol. 43, no. 2, pp.347–354, Apr. 1994.

[30] J. Verspecht, " Compensation of timing jitter-induced distortion of sampled waveforms," *IEEE Trans. Instrum, Meas.,* vol. 43, no. 5, pp.726–732, Oct. 1994.

[31] P. Ferrari and G. Angenieux, "A simulation technique for the evaluation of random error effects in time domain measurement systems," *IEEE Trans. Instrum, Meas.,* vol. 50, no. 3. pp. 665–671, Jun. 2001.

[32] P. D. Hale, C. M. Wang, D. F. Williams, K. A. Remley and J. D. Wepman, "Compensation of random and systematic timing errors in sampling oscilloscopes," *IEEE Trans. Instrum, Meas.,* vol. 55, no. 6, pp. 2146–2154, Dec. 2006.

[33] G. W. Stimson *Introduction to Airborne Radar*, SciTech Publishing, 1998.

[34] J. R. Andrews, "Removing jitter from picosecond pulse measurments," *Application Note AN-23,* Picosecond Pulse Labs, Boulder, CO, 2009.

[35] Agilent PNA Microwave Network Analyzers (Data Sheet). *http://www.home.agilent.com/*

[36] Evaluating Ocilloscope Bandwidths for your Application–Application Note 1588. *http://www.home.agilent.com/*

[37] HP 54750A High-Bandwidth Digitizing Oscilloscope–Product Overview. *http://www.airlink.dk/Dokumenter/HP54750A.pdf.*

[38] B. Widrow and I. Kollar *Quantization Noise: Roundoff Error in Digital Computation, Signal Processing, Control, and Communications.* Cambridge University Press, Cambridge, UK, 2008.

[39] Digital Serial Analyzer Sampling Oscilloscope DSA8200. *http://www.tek.com/products/oscilloscopes/dsa8200.*

[40] WaveExpert Sampling Oscilloscopes WaveExpert 100H. *http://www.lecroy.com.*

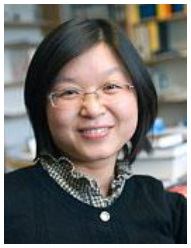

Xuezhi Zeng was born in 1980 in China. She received the M.Sc. degree in electrical engineering in 2006 from Jiangsu University, Zhenjiang, China. She is currently working towards the Ph.D. degree at Chalmers University of Technology, Göteborg, Sweden. Her research interests include electromagnetic imaging, antenna design, microwave measurement and system design.

Andreas Fhager was born in 1976 in Sweden. He received the M.Sc. degree in engineering physics from Chalmers University of Technology, Göteborg, Sweden in 2001. In 2004 he received the Licentiate of Technology degree in microwave imaging and in 2006 he received the Ph.D. degree in the same field at Chalmers. Currently he is working as an assistant professor at Chalmers. His research interests include electromagnetic imaging methods for breast cancer detection and other biomedical applications of microwaves.

Peter Linner (S'69-M'74-SM'87-LSM'10) In 1969 he became a Teaching Assistant in mathematics and telecommunications at Chalmers University of Technology. In 1973 he joined the research and teaching staff of the Division of Network Theory at the same university with research interests in the areas of network theory, microwave engineering, and computer-aided design methods. In 1974 he moved to the MI-division, Ericsson Telephone Company, Mölndal, Sweden, where he was a systems engineer and project leader in several military radar projects. He returned to Chalmers University of Technology as a Researcher in the areas of microwave array antenna systems. Since 1981 he has been an Associate Professor in telecommunications. For part of 1992 he spent a period at University of Bochum, Bochum, Germany as a Guest Researcher. His current interest is in the application of computer-aided network methods, microwave circuit technology with emphasis on filters, matching, modeling, and lumped-element methods.

Mikael Persson received his MSc and PhD degree from Chalmers University of Technology, Göteborg, Sweden, in 1982 and 1987, respectively. In 2000 he became professor of Electromagnetics and in 2006 Professor in Biomedical Electromagnetics at the Department of Signal and Systems, in Chalmers University of Technology. He is presently the head of the Division of Signal Processing and Biomedical engineering and the director for the regional research and development platform MedTech West. At present these activities involve approximately 50 researchers. His main research interests include electromagnetic diagnostics and treatment. He is author/co-author of more than 200 refereed journal and conference papers.

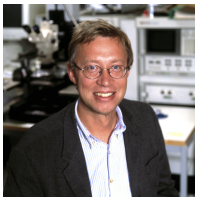

Herbert Zirath received his MSc and PhD degree from Chalmers University of Technology, Göteborg, Sweden, in 1980 and 1986, respectively. He is since 1996 a Professor in High Speed Electronics at the Department of Microtechnology and Nanoscience, MC2, in Chalmers University of Technology. He became the head of the Microwave Electronics Laboratory during 2001. At present he is leading a group of approximately 50 researchers in the area of high frequency semiconductor devices and circuits. His main research interests include foundry related MMIC designs for millimeterwave applications based on both III-V and silicon devices, SiC and GaN based transistors and circuits for high power applications, device modeling including noise and large-signal models for FET and bipolar devices, and InP-HEMT devices and circuits. He is working part-time at Ericsson AB as a microwave circuit expert. He is author/co-author of more than 300 refereed journal/conference papers, and holds 4 patents. He is an IEEE-fellow.